SURFACE AND INTERFACE ANALYSIS, VOL. 14, 730–738 (1989)

Non-destructive Depth Profiling Through Quantitative Analysis of Surface Electron Spectra

S. Tougaard and H. S. Hansen
Fysisk Institut, Odense Universitet, DK-5230 Odense M, Denmark

A theory is presented that allows detailed quantitative information on in-depth concentration profiles to be extracted through analysis of surface electron spectra. The depth profile is determined from analysis of a single spectrum and the method is therefore fast and non-destructive. The validity of the method is tested through analysis of model spectra from a wide variety of inhomogeneous systems. It is demonstrated that the method can clearly distinguish between different classes of in-depth profiles. Moreover, the formalism can be used to distinguish between different overlayer growth mechanisms. The resolution in the determination of the detailed concentration depth profile is of the order of the inelastic mean free path λ. The accuracy of the total amount of material within depths of 4–6 λ determined by the analysis is, in all cases, better than 10–15%.

INTRODUCTION

Quantitative analysis of Auger electron and x-ray photoelectron spectra (AES and XPS) is complicated by the elastic and inelastic scattering processes that take place during the transport of the excited electrons out of the solid.

The influence of elastic scattering has been studied analytically[1–3] and in several numerical Monte Carlo-based calculations.[4–7] Thus, it was shown that the measured peak intensity, as well as the angular distribution of emitted electrons, is affected by elastic electron scattering.

Inelastic scattering processes will cause the energy distribution of emitted electrons to be distorted in comparison with the energy distribution at the point of excitation in the solid. A measured spectrum must be corrected for this effect before any quantitative analysis can be performed. The problem has been investigated in a number of papers,[1,8–10] where a physical model was defined. Based on this, a simple formula was found, which was shown to be approximately valid for inelastic background correction of spectra originating from samples with a wide class of in-depth concentration profiles.[10] Being extremely simple, this formula is useful as a routine method for spectral analysis. However, in situations where a more exact analysis is required, at the expense of extra time and effort, more accurate formulas are needed. Previously, exact formulas were found for analysis of spectra from samples with two types of in-depth concentration profiles, namely a constant[1] and an exponentially varying depth distribution.[11] In addition, an approximate formula was found for a sharp depth distribution of electron emitters.[12]

In the present work, a general formula valid for any in-depth concentration profile is derived. The formula is more complicated in comparison with the previous formulas, since it involves several infinite integrals. However, it is shown that the integrals can be converted into a form that is well suited for evaluation by fast Fourier transformation (FFT). It is found that for several classes of in-depth concentration profiles, one of the integrations in the formula can be performed analytically, with a resulting reduction in the numerical calculations.

The validity of the formalism is demonstrated for theoretical spectra from various in-depth profiles.

It was previously shown that the detailed shape of the inelastic background does contain valuable information on the in-depth concentration profile.[13,14] Thus, through analysis of the ratio of the peak area to the increase in background signal associated with the peak, information on the concentration profile is readily obtained. The method does not give the detailed in-depth concentration profile, and some *a priori* information on the type of distribution is, in general, required. However, since the method is so simple and the information is so easily extracted, it is obvious that advantage be taken of this extra in-depth information.

Much more detail on the depth profile can be extracted by the more complicated method presented here. Thus, since the formulas derived in the present work depend critically on the in-depth concentration profile, analysis of the peak shape does give quite detailed quantitative information on the in-depth concentration profile. In addition to this, the present formalism can give direct information on the detailed growth mechanism of one element on another through analysis of the shape of XPS peaks. As an example, it is demonstrated that the formalism through analysis of a single spectrum can decide whether an overlayer growth proceeds layer by layer or through island formation. Simultaneously, the growth is determined quantitatively.

We are currently studying spectra from experimentally produced inhomogeneous systems.[15] The conclusions concerning the validity of the formalism are quite similar to those drawn here on the basis of theoretical model spectra.

0142-2421/89/110730-09 $05.00

Received 21 March 1989
Accepted 16 June 1989

The time needed for analysis of a spectrum with 500 data points on a standard APOLLO computer is typically <15 s.

2. THEORY

In the present section, we derive a general formula to correct for the distortion of an electron energy spectrum caused by inelastic electron scattering. For a given spectrum, the amount of distortion will depend on two fundamental quantities, namely the cross-section for inelastic scattering and the distribution of path lengths experienced by the excited electrons prior to emission. Realistic models for the inelastic scattering cross-section have been published previously.[8,16,17] The path length distribution of emitted electrons depends first of all on the in-depth concentration profile of the corresponding element. Elastic scattering may cause the electron path to deviated from a straight line,[1–7] as demonstrated by Jablonski in several Monte Carlo simulations.[6,7] No general analytical formula is available to describe this effect. However, since in general the transport mean free path for elastic scattering is larger than the mean free path for inelastic electron scattering, the effect of elastic scattering on the spectrum of emitted electrons is expected to be small. Therefore, an accurate description of inelastic scattering is far more important for a description of the energy distribution of emitted electrons in the near-peak region compared to the effect on the path length distribution of emitted electrons implied by angular deflection owing to elastic scattering.[8] Thus, the influence of elastic scattering on the energy spectra in the near-peak region is likely to be smaller than the influence caused by the uncertainty on available inelastic mean free path data.

Therefore, we shall neglect here the angular electron deflection and assume that the electrons move along straight lines. Future developments in the description of angular deflection may be incorporated easily in the present formalism.

The formalism presented here is valid for the analysis of both XPS and AES. However, in electron-stimulated AES, back-scattering effects may cause the excitation to be slightly non-uniform in the surface region of the solid. This may, if necessary, be taken into account in the interpretation of the concentration depth profile determined from analysis of AES by the present formalism.[8] A similar problem does not exist in XPS since the attenuation length of the x-rays is much larger than the depths involved here.

2.1. General formula

Let $F(E_0, \Omega_D, x)\, dE_0\, dx$ be the flux of electrons excited at depth x, dx in an energy interval E_0, dE_0 into the solid angle Ω_D of the detector. Let us assume that the concentration of electron emitters $f(x)$ may vary with depth x but that the energy distribution is independent of depth, i.e.

$$F(E_0, \Omega_D, x) = f(x)F(E_0, \Omega_D) \tag{1}$$

where $F(E_0, \Omega_D)$ is the number of electrons per second, per atom and per unit energy emitted into the solid angle Ω_D of the detector, while $f(x)$ is the number of atoms per Å at depth x. Then the number of electrons $J(E, \Omega_D)$ emitted per second and per unit energy from the solid surface into the solid angle Ω_D is given by[1,8]

$$J(E, \Omega_D) = \frac{1}{2\pi}\int dE_0\, F(E_0, \Omega_D)\int ds\, \exp(is(E_0 - E)) \times \int dx f(x)\exp\left[-\frac{x}{\cos\theta}\Sigma(s)\right] \tag{2}$$

where θ is the angle between the surface normal and detector.

In Eqn (2)

$$\Sigma(s) = \frac{1}{\lambda} - \int_0^\infty K(T)\exp(-isT)\, dT \tag{3}$$

where λ is the mean free path for inelastic electron scattering and $K(T)$ is the differential inelastic scattering cross-section i.e. the probability that an electron shall lose energy T per unit energy loss and per unit path length travelled in the solid.

The objective is now to solve the integral equation, Eqn (2), for $F(E_0, \Omega_D)$, assuming that $f(x)$ is known. To this end, Eqn (2) is first Fourier-inverted with respect to E and we find

$$\int dx f(x)\exp\left[\frac{-x}{\cos\theta}\Sigma(s')\right]\int dE_0\, F(E_0, \Omega_D)\exp(is'E_0) = \int J(E, \Omega_D)\exp(is'E)\, dE \tag{4}$$

Then

$$\int dE_0\, F(E_0, \Omega_D)\exp(is'E_0) = \frac{1}{\int dx f(x)\exp\left[-\frac{x}{\cos\theta}\Sigma(s')\right]}\int J(E, \Omega_D)\exp(is'E)\, dE \tag{5}$$

After Fourier transformation with respect to s' and insertion of Eqn (3), we finally find

$$F(E, \Omega_D) = \frac{1}{2\pi}\int dE' J(E', \Omega_D)\int ds \times \exp[-is(E - E')]\frac{1}{P(s)} \tag{6}$$

where

$$P(s) = \int_0^\infty f(x)\exp\left[-\frac{x}{\cos\theta}\Sigma(s)\right]dx \tag{7}$$

Equation (6) is a solution of the desired form. The formula is exact under the assumptions made above.

In Eqn (6), $J(E, \Omega_D)$ is the measured spectrum. The inelastic mean free path λ needed in the evaluation of $\Sigma(s)$ (Eqn (3)) may be estimated from one of the various published tabulations.[18–20] For $K(T)$ we may, for many solids, use the 'universal' cross-section[17]

$$K(T) \simeq \frac{1}{\lambda}\frac{B \cdot T}{(C + T^2)^2} \tag{8}$$

where $C \simeq 1643$ eV^2 and $B \simeq 2866$ eV^2.

Alternatively, $K(T)$ may be evaluated within a dielectric response description[16,21] or through a simple analysis of a spectrum of back-reflected electrons.[22] In the present work, we shall exclusively use Eqn (8). This is also shown to be sufficiently accurate in the analysis of experimental spectra by Eqn (6).[15]

Now, the only unknown quantity in Eqn (6) is the in-depth concentration profile $f(x)$. On the low kinetic energy side of a given peak, $F(E)$ is known to decrease rapidly, and beyond 40–50 eV from the peak, $F(E) \simeq 0$.[23] Then, Eqn (6) may be used to determine the in-depth concentration profile of an element by the requirement that $F(E) \simeq 0$ in a wide energy range below the corresponding peak. If more than one spectrum enters in the analysis, it is further required that the $F(E)$ values obtained are consistent on an absolute scale. For a more accurate analysis, $F(E)$ may first be determined from a sample of the pure metal. Then, the analysis by Eqn (6) is carried out with the requirement that the resulting $F(E)$ on an absolute scale is close to the $F(E)$ obtained from analysis of the homogeneous sample (see also Section 4).

Note that $\Sigma(s)$ and $P(s)$ are the Fourier transforms of energy distribution functions. They are introduced solely for mathematical convenience and have no direct physical significance. For instance, assuming $F(E_0, \Omega_D) \propto \delta(E - E_0)$, then $P(s)$ will be the Fourier transform of the spectrum of emitted electrons.

2.2. Numerical evaluation of the integrals

To evaluate Eqn (6) for a given depth profile, $f(x)$, $\Sigma(s)$ and $P(s)$ given by the integrals in Eqns (3) and (7) must first be evaluated.

Since $K(T) = 0$ for $T \leqslant 0$ and since $K(T)$ is well behaved for $T > 0$ (see Eqn (8)), $\Sigma(s)$ can be approximated by its discrete Fourier transform and evaluated numerically by fast Fourier transformation.[24] $P(s)$, given by Eqn (7), may be evaluated by standard numerical methods or, in certain cases, even analytically (see below), provided that $f(x)$ is known.

Finally, to put Eqn (6) into a form suitable for discrete Fourier transformation, we define

$$P_1 = \int_0^\infty f(x) \exp\left(\frac{-x}{\lambda \cos\theta}\right) dx \tag{9}$$

Then, Eqn (6) may be written

$$F(E, \Omega_D) = \frac{1}{P_1}\left\{J(E, \Omega_D) - \frac{1}{2\pi}\int dE' J(E', \Omega_D) \int ds \times \exp[-is(E - E')]\left[1 - \frac{P_1}{P(s)}\right]\right\} \tag{10}$$

Since $P_1 = \lim_{s \to \pm\infty} P(s)$, $1 - P_1/P(s) \to 0$ for $s \to \pm\infty$ and the function $1 - P_1/P(s)$ is suitable for discrete Fourier transformation.[24]

The integral over s in Eqn (10) is then evaluated by fast Fourier transformation. The integral over E' in Eqn (10), as well as P_1 (Eqn (9)), is easily evaluated numerically and $F(E, \Omega_D)$ is then determined.

For a general in-depth concentration profile given by $f(x)$, Eqn (10) can be used directly (see Section 4). However, it is found that for several classes of depth profiles, the integral over x in the expressions for P_1 and $P(s)$ can be performed analytically. This will reduce the time required for the numerical evaluation. Such examples are considered in the following section.

3. P_1 AND $P(s)$ FOR SPECIAL CLASSES OF DEPTH PROFILES $f(x)$

3.1. Homogeneous and exponential depth profiles

For $f(x) = c \exp(-x/L)$, we find

$$P_1 = c\frac{\lambda L \cos\theta}{L + \lambda \cos\theta} \tag{11}$$

$$P(s) = c\frac{L \cos\theta}{L \cdot \Sigma(s) + \cos\theta} \tag{12}$$

In this case, the integral over s in Eqn (10) can also be performed analytically to give

$$F(E, \Omega_D) = \frac{L + \lambda \cos\theta}{c\lambda L \cos\theta}\left[J(E, \Omega_D) - \frac{\lambda L}{L + \lambda \cos\theta} \times \int_E^\infty dE' J(E', \Omega_D) K(E' - E)\right] \tag{13}$$

This result was obtained previously.[11]

3.2. $f(x) = N\delta(x - X_0)$

Here, N is the total number of atoms, all at depth X_0, and we find from Eqns (7) and (9)

$$P_1 = N \exp\left(-\frac{X_0}{\lambda \cos\theta}\right) \tag{14}$$

$$P(s) = N \exp\left(-X_0 \frac{\Sigma(s)}{\cos\theta}\right) \tag{15}$$

3.3. Box-shaped profiles (overlayer, substrate and sandwich, see Fig. 1)

First, we consider the sandwich profile, since formulas for analysis of spectra from an overlayer and the corresponding substrate are obtained from this as limiting cases.

Let us assume that the sandwich profile consists of two elements, as shown in Fig. 1. (Extension to more than two elements is straightforward.) For one of the elements we have, $f(x) = c$ for $X_0 < x < X_0 + DX$,

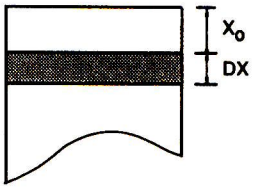

Figure 1. Schematic showing a box-shaped depth profile.

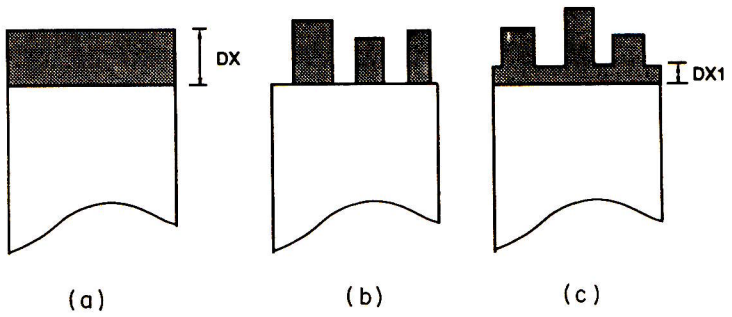

Figure 2. Schematic showing three different possible overlayer growth mechanisms.

while $f(x) = 0$ otherwise. Then, from Eqns (7) and (9)

$$P_1 = c \cdot \lambda \cdot \cos\theta \cdot \exp\left(-\frac{X_0}{\lambda \cos\theta}\right) \times \left[1 - \exp\left(-\frac{DX}{\lambda \cos\theta}\right)\right] \quad (16)$$

$$P(s) = c \cdot \frac{\cos\theta}{\Sigma(s)} \cdot \exp\left(-X_0 \cdot \frac{\Sigma(s)}{\cos\theta}\right) \times \left[1 - \exp\left(-DX\,\frac{\Sigma(s)}{\cos\theta}\right)\right] \quad (17)$$

For the other element, $f(x) = c$ for $0 < x < X_0$ and $X_0 + DX < x$, while $f(x) = 0$ otherwise. Then, from Eqns (7) and (9) we get

$$P_1 = c \cdot \lambda \cdot \cos\theta \left\{1 - \exp\left(-\frac{X_0}{\lambda \cos\theta}\right) \times \left[1 - \exp\left(-\frac{DX}{\lambda \cos\theta}\right)\right]\right\} \quad (18)$$

$$P(s) = c \cdot \frac{\cos\theta}{\Sigma(s)} \left\{1 - \exp\left(-X_0 \cdot \frac{\Sigma(s)}{\cos\theta}\right) \times \left[1 - \exp\left(-DX\,\frac{\Sigma(s)}{\cos\theta}\right)\right]\right\} \quad (19)$$

Now, expressions for P_1 and $P(s)$ for analysis of spectra from an overlayer and substrate are readily obtained by setting $X_0 = 0$ in Eqns (16) and (17) and Eqns (18) and (19), respectively.

3.4. Other classes of concentration depth profiles

Analytical expressions for P_1 and $P(s)$ are also obtained easily for other classes of depth profiles, as for instance multiple alternating layers, and an exponential depth profile superimposed on a constant concentration. If a depth profile is examined for which analytical evaluation of P_1 and $P(s)$ is not possible, Eqn (10) can always be applied directly, since the integrals involved in the expressions for P_1 and $P(s)$ are easily evaluated numerically.

3.5. Determination of overlayer growth mechanism

Various modes of growth of an overlayer on a substrate have been identified.[25] They include layer-by-layer growth (Frank–van der Merwe), island growth (Volmer–Weber) and layer-by-layer plus island growth (Stranski–Krastanov). Alternatively, the overlayer may diffuse into the substrate. The various possibilities are illustrated schematically in Fig. 2. Since these growth modes are the most frequently observed for experimental systems, we shall derive explicit expressions for each one of them.

Layer-by-layer growth (Fig. 2(a)). This is identical to the box-shaped profile treated in Section 3.3 with $X_0 = 0$.

Layer-by-layer plus island growth (Fig. 2(c)). In the general case, both the height and the width of the islands are given by distribution functions. This general case may be treated by Eqn (10). If we assume that the island height can be approximated by their mean height DX (see Fig. 3(a)) then this is, for normal electron emission from the point of view of the spectral shape, identical to the profile shown in Fig. 3(b) which effectively is the same as the profile shown in Fig. 3(c).

Note that for non-normal emission, Fig. 3(a) and (c) are not strictly identical, since some electrons may hit the islands on their way to the detector. For normal or near-normal emission, the effect will be negligible.

Now, for the overlayer, $f(x) = c$ for $0 < X < DX1$ and $f(x) = cf_1$ for $DX1 < x < DX$, while $f(x) = 0$ otherwise. Here, f_1 is the fractional surface coverage ($0 \leqslant$

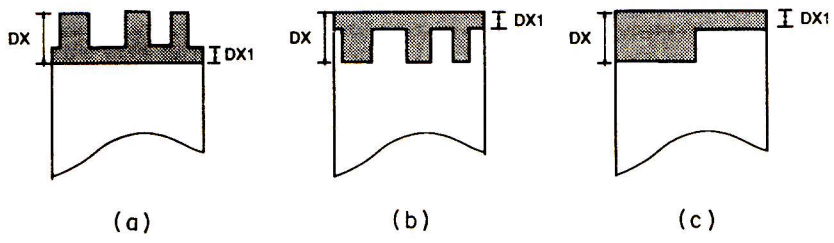

Figure 3. For a near-normal exit, the spectral shape from both substrate and overlayer will be identical for the three profiles (a), (b) and (c) (see text).

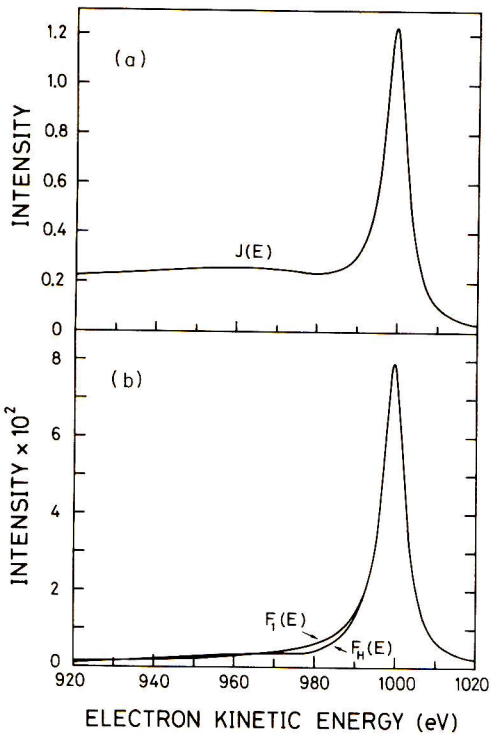

Figure 4. (a) Spectrum $J(E)$ from a homogeneous gold sample. (b) Primary spectrum $F_H(E)$ after analysis by Eqn (13) with $L = \infty$ and $c = 1$. Also shown is the true primary spectrum $F_1(E)$.

$f_1 \leqslant 1$). Then, from Eqns (7) and (9)

$$P_1 = c \cdot \lambda \cdot \cos\theta\left[1 - (1 - f_1)\exp\left(-\frac{DX1}{\lambda \cos\theta}\right) - f_1 \exp\left(-\frac{DX}{\lambda \cos\theta}\right)\right] \quad (20)$$

$$P(s) = c \cdot \frac{\cos\theta}{\Sigma(s)}\left[1 - (1 - f_1)\exp\left(-DX1\,\frac{\Sigma(s)}{\cos\theta}\right) - f_1 \exp\left(-DX\,\frac{\Sigma(s)}{\cos\theta}\right)\right] \quad (21)$$

For the substrate, $f(x) = c(1 - f_1)$ for $DX1 < x < DX$ and $f(x) = c$ for $DX < x$, while $f(x) = 0$ otherwise. Then Eqns (7) and (9) give

$$P_1 = c \cdot \lambda \cdot \cos\theta\left[(1 - f_1)\exp\left(-\frac{DX1}{\lambda \cos\theta}\right) + f_1 \exp\left(-\frac{DX}{\lambda \cos\theta}\right)\right] \quad (22)$$

$$P(s) = c \cdot \frac{\cos\theta}{\Sigma(s)}\left[(1 - f_1)\exp\left(-DX1\,\frac{\Sigma(s)}{\cos\theta}\right) + f_1 \exp\left(-DX\,\frac{\Sigma(s)}{\cos\theta}\right)\right] \quad (23)$$

Island growth (Fig. 2(b)). This is a special case of the layer-by-layer plus island growth treated above with $DX1 = 0$. As before, these formulas are valid under the assumption that the distribution of island heights can be approximated by its mean value.

Diffusion of overlayer into substrate and formation of alloys. The overlayer may diffuse into the substrate to form a region of width DX of a stoichiometric compound. This is, from the point of view of the spectral shape, identical to island growth, i.e. Eqns (20)–(23) with $DX1 = 0$, except that it will hold here for any emission angle. Alternatively, the diffusion profile may be exponential, in which case the simpler formula, Eqn (13), applies. For more general diffusion profiles, the general formula, Eqn (10), may always be applied.

4. EXAMPLES AND DISCUSSION

In this section we analyse theoretical XPS spectra from samples with various types of in-depth concentration profiles. We are currently studying measured spectra from experimentally produced systems of inhomogeneous samples.[15] The conclusions from these experimental investigations concerning the validity of the method presented here are quite similar to those drawn in this section from analysis of theoretical spectra.

The theoretical spectra were evaluated for a detection angle normal to the surface ($\theta = 0$) by a method described previously.[8,11] Input in the calculations are the following: the primary spectrum, denoted by $F_1(E)$, is taken to be of the Doniach–Sunjic form[26] with $\alpha = 0.1$ and $\gamma = 3.0$ eV centred around 1000 eV. The material was, in all cases, gold and the cross-section $K(T)$ was evaluated on the basis of a dielectric response calculation.[8,16] The concentration depth profile was varied as described below.

Subsequently, the spectra $J(E)$ thus obtained were analysed by the formulas in Section 3. If, in this analysis, the same cross-section is used as in the evaluation of the theoretical spectra, the resulting primary spectra $F(E)$ are always found to be practically identical to the true primary spectra $F_1(E)$. This illustrates that the error in the numerical evaluation of the involved integrals is negligible. However, in analysis of experimental spectra from a general sample, the exact $K(T)$ function is never known. To imitate this situation, the 'universal' cross-section (Eqn (8), with $\lambda = 15.25$ Å for Au at 1000 eV[18]) was applied rather than the exact cross-section used in the evaluation of the spectra. This will introduce an uncertainty in $K(T)$, which is always present in the analysis of experimental spectra.

In all the formulas of the previous section, $f(x)$ is given as a constant c multiplied by a form factor. From analysis of a single spectrum, the form factor of $f(x)$ can be determined (by the requirement that $F(E) \simeq 0$ in a wide energy range, e.g. from 40 to 100 eV, below the peak energy). If the spectrum of a sample with a well-known depth distribution (e.g. a pure homogeneous sample) is also included in the analysis, the constant c is also determined from the analysis (by the requirement that $F(E)$ is close to $F(E)$ obtained from the homogeneous sample) and $f(x)$ is then determined on an absolute scale. If we choose $c = 1$ in the analysis of the spectrum from a homogeneous sample, then $f(x)$ resulting from analysis of a given spectrum will be in fractions of the concentration of the pure material.

Figure 4(a) shows a spectrum $J(E)$ evaluated for a homogeneous gold sample. After analysis by Eqn (13) with $L = \infty$ and $c = 1$, we get the lower spectrum $F_H(E)$ in Fig. 4(b), which is quite close to the true primary

spectrum $F_1(E)$. The deviations are exclusively due to the difference between the universal cross-section (Eqn (8)) and the dielectric-response-calculated cross-section used in the evaluation of the spectrum $J(E)$.

Now, in the analysis of spectra from the various concentration depth profiles studied below, a class of depth profiles $f(x)$ is first chosen (e.g. box-shaped profile). The parameters describing this profile are then adjusted to give the same peak height in $F(E)$ as is observed in $F_H(E)$ from the analysis of the pure gold sample in Fig. 4(b). In situations where chemically induced changes in peak shape occur, the peak area rather than the peak height should be used as a criterion. After analysis, the shape of the low-energy tail is compared to $F_H(E)$. If they differ, the assumed model $f(x)$ was wrong and another class of $f(x)$ must be considered. For future routine applications of the present method, a comparison based on minimizing the least-squares difference between $F(E)$ and $F_H(E)$ may be used to automate the fitting procedure.

In Fig. 5(a) we consider spectra $J(E)$ from gold overlayers of thickness 10, 20 and 40 Å. After analysis by Eqn (10), using Eqns (16) and (17) with $X_0 = 0$, the background-corrected spectra $F(E)$ in Fig. 5(b) were obtained by adjusting the overlayer thickness DX to yield the same peak intensity as $F_H(E)$. The thicknesses thus obtained are 10.0, 20.0 and 38.5 Å, respectively.

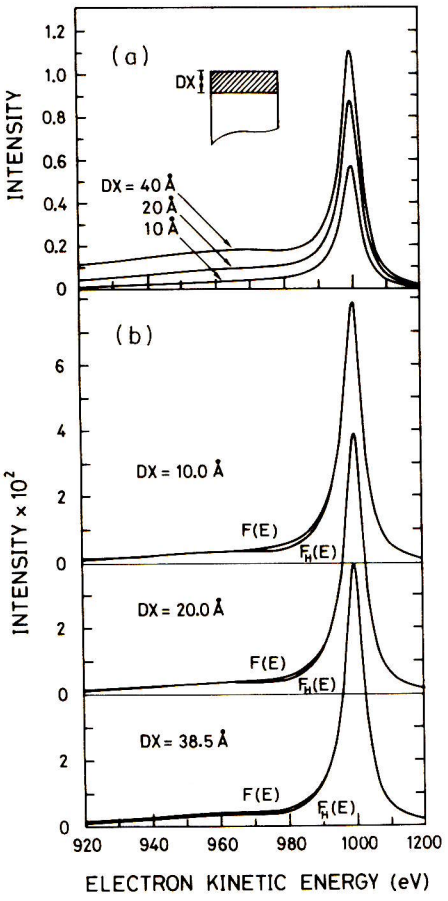

Figure 5. (a) Spectrum from a gold overlayer of width $DX = 10$, 20 and 40 Å. (b) Primary spectra $F(E)$ after analysis by Eqn (10) using Eqns (16) and (17) with $X_0 = 0$, adjusting the overlayer thickness DX to give the same absolute peak intensity in $F(E)$ as in $F_H(E)$.

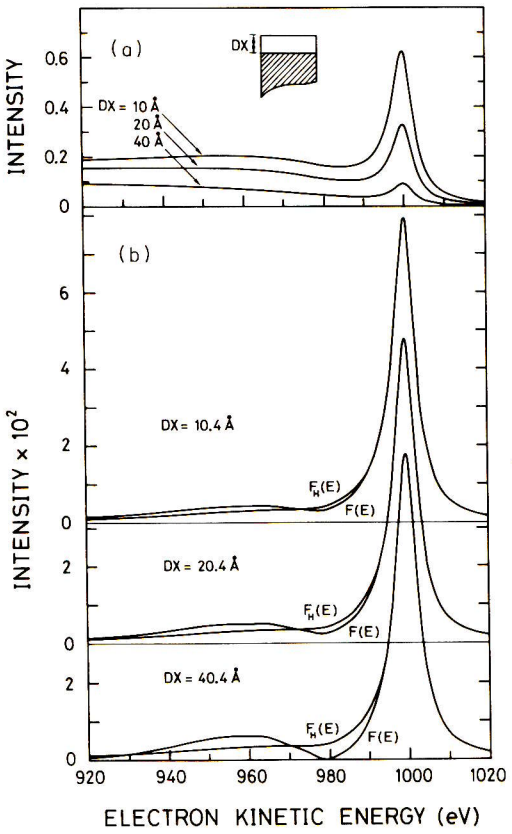

Figure 6. (a) Spectra from a gold substrate with an overlayer of thickness 10, 20 and 40 Å, respectively. (b) Primary spectra $F(E)$ obtained by Eqn (10) using Eqns (18) and (19) with $X_0 = 0$. DX was adjusted to give the same peak intensity in the background-corrected spectra $F(E)$ as in $F_H(E)$.

For comparison, $F_H(E)$ from the analysis of the homogeneous sample (Fig. 4) is also shown.

In Fig. 6(a) we consider spectra from a gold substrate with overlayers of thickness 10, 20 and 40 Å. The spectra were analysed (see Fig. 6(b)) by Eqn (10) using Eqns (18) and (19) with $X_0 = 0$. DX was adjusted to give the same peak intensity in the background-corrected spectra $F(E)$ as in $F_H(E)$. The resulting thickness is $DX = 10.4$, 20.4 and 40.4 Å, respectively.

The detailed shape of the primary spectra $F(E)$ in Figs 5 and 6 are, in all cases, very close to $F_H(E)$. The largest deviation is observed for the spectrum from a substrate with a 40 Å overlayer. This deviation is not due to a numerical error in the evaluation of the integrals, since an evaluation based on the exact $K(T)$ yields the correct primary spectrum. The deviation observed for large overlayers is due to the slightly incorrect cross-section used in the analysis. The same trend is observed in the analysis of experimental spectra.[15]

In addition to a determination of the background-corrected spectra, the present analysis also gives quantitative information on the in-depth concentration profile. In fact, for all six spectra in Figs 5 and 6, the overlayer thicknesses obtained from the analysis are very close to the exact values.

To summarize, in the practical application of the present formalism, a specific class of depth profiles is first chosen. Then, the parameters describing this class are varied to give either a zero in a wide energy range

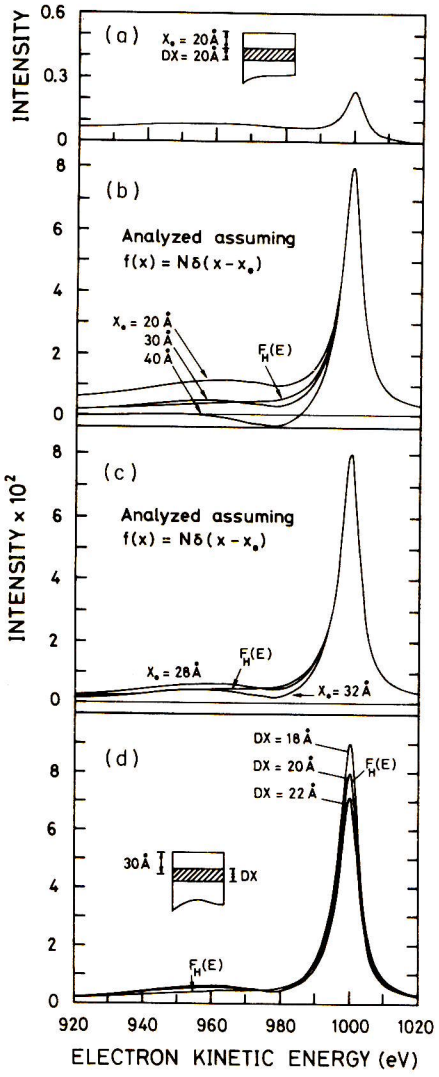

Figure 7. (a) Spectrum from a sandwich structure consisting of a 20 Å wide gold layer with an overlayer of 20 Å. In (b) and (c) this spectrum is analysed assuming $f(x) = N\,\delta(X - X_0)$ by Eqn (10) using Eqns (14) and (15) under variation of X_0 and N. For X_0 = 20, 28, 30, 32 and 40 Å, N = 11.1, 18.5, 21.0, 24.0 and 40.0, respectively. In (d), the width of the distribution is varied, keeping the centre fixed at 30 Å depth. Thus, the spectrum is analysed by Eqn (10) using Eqns (16) and (17) under variation of DX.

below the peak or to match $F_H(E)$. If this is not possible, another class of depth profiles must be considered.

As an example of how this may be done in practice, we consider in Fig. 7 a spectrum from a sandwich structure consisting of a 20 Å wide gold layer with an overlayer of 20 Å (see insert in Fig. 7(a)). This spectrum is first analysed by assuming a narrow depth distribution given by $f(x) = N\,\delta(X - X_0)$. To this end, Eqn (10), with Eqns (14) and (15), was used under variation of X_0 and N. In this analysis, X_0 will determine the shape of $F(E)$, while N acts as a scaling factor. For X_0 = 30 Å, $F(E)$ is quite close to $F_H(E)$ (see Fig. 7(b)). Figure 7(c) shows that we can clearly discriminate between X_0 = 28, 30 and 32 Å. For X_0 = 20, 28, 30, 32 and 40 Å, N = 11.1, 18.5, 21.0, 24.0 and 40.0, respectively. Now, although X_0 = 30 Å with N = 21.0 gives an acceptable agreement between $F(E)$ and $F_H(E)$, this value of N is unacceptable, since it implies that the density of gold atoms at X = 30 Å would be 21 times larger than in a pure gold sample. Therefore, the width of the distribution was now varied keeping the centre fixed at 30 Å depth. Thus, the spectrum is now analysed by Eqn (10) using Eqns (16) and (17) with c = 1 under variation of DX. The results for DX = 18, 20 and 22 Å are shown in Fig. 7(d) and are compared on an absolute scale to $F_H(E)$ from a homogeneous sample (Fig. 4(b)). For DX = 20 Å, the peak height is exactly that of $F_H(E)$ and the concentration depth profile is thus determined to be a sandwich of width 20 ± 2 Å with an overlayer of width 20 ± 1 Å. This result is very close to the actual depth composition profile. Note that only two experimental spectra are needed to obtain this detailed information on the in-depth concentration profile.

Finally, we illustrate that the present formalism can be used to discriminate between different overlayer growth mechanisms. Let us assume that an overlayer grows on a substrate by the formation of islands, which cover a 50% fraction of the surface. Let us assume that deposition of material on the surface is terminated when the island height is 40 Å. The resulting structure is shown in the insert in Fig. 8(a). The spectra from the overlayer and the substrate are shown in Figs 8(a) and 9(a) respectively.

Now, these spectra were first analysed by assuming a layer-by-layer growth, i.e. Eqn (10) with Eqns (20) and (21) for Fig. 8 and Eqns (22) and (23) for Fig. 9. In both cases, $DX1 = 0$ and $f_1 = 1.00$. (Alternatively, we could have used Eqns (16)–(19) with exactly the same result, since for $X_0 = 0$ they are identical to Eqns (20)–(23) with $f_1 = 1$ and $DX1 = 0$.) After adjusting DX to yield the same absolute peak height as in $F_H(E)$, we obtain the primary spectra marked (1) in Figs 8(b) and 9(b) for the overlayer and the substrate spectra, respectively. These spectra are both markedly different from $F_H(E)$ in the region below the peaks. The conclusion then is that the overlayer growth does not proceed layer by layer.

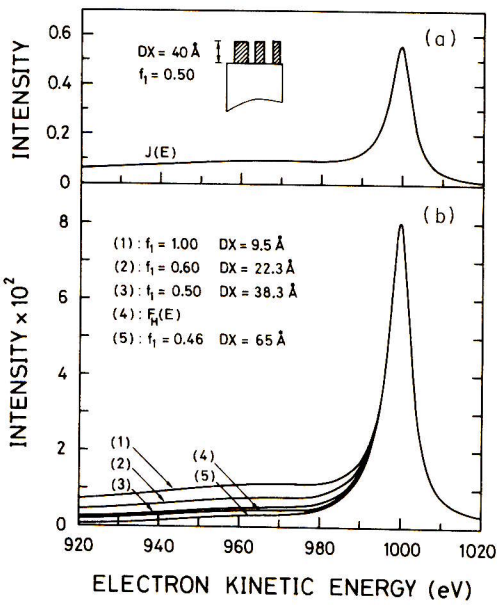

Figure 8. (a) Spectrum from a gold overlayer that is assumed to grow on a substrate by the formation of islands covering a 50% fraction of the surface. (b) Analysis of the spectra in (a), assuming island growth, i.e. Eqn (10) with Eqns (22) and (23) with f_1 = 1.00, 0.60, 0.50 and 0.46, respectively. In each case, the island height DX was adjusted to give equal peak heights in $F(E)$ and $F_H(E)$.

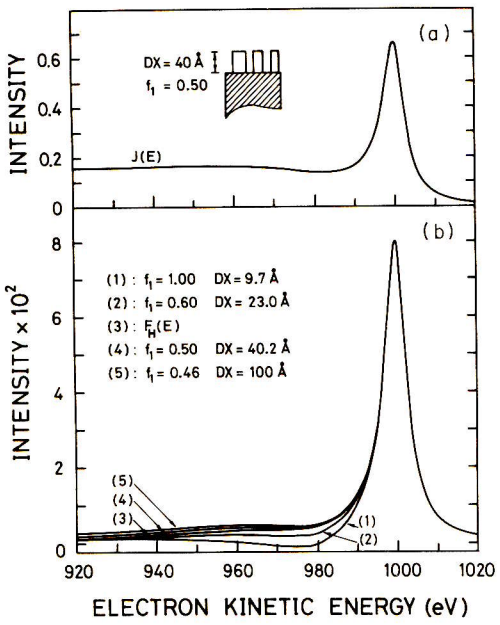

Figure 9. (a) Spectrum from a gold substrate with an overlayer that is assumed to grow by the formation of islands covering a 50% fraction of the surface. (b) Analysis of the spectra in (a), assuming island growth, i.e. Eqn (10) with Eqns (22) and (23) with $f_1 = 1.00$, 0.60, 0.50 and 0.46, respectively. In each case, the island height DX was adjusted to give equal peak heights in $F(E)$ and $F_H(E)$.

Next, we assume island formation with a fractional surface coverage of $f_1 = 0.60$, 0.50 and 0.46, respectively. In each case, the island height DX was adjusted to give equal peak heights in $F(E)$ and $F_H(E)$, as shown in Figs 8(b) and 9(b). The best agreement is obtained in both cases for $f_1 = 0.50$ and the resulting island heights as determined from the overlayer and substrate spectra are $DX = 38.3$ Å and $DX = 40.2$ Å, respectively. The conclusion is that the overlayer forms islands with a 50% surface coverage and an island height of $DX = 39 \pm 2$ Å. This is very close to the actual surface structure.

Note that these quite detailed results on overlayer growth mechanism are obtained through a rather simple analysis of only two spectra: namely, the spectrum from the pure sample and from either the overlayer or the substrate of the sample under investigation.

Finally, we make some remarks on the accuracy of the method. If $K(T)$ and $J(E)$ were known with sufficient accuracy, it would in principle be possible to determine the exact surface structure. However, in practice, the accuracy will be limited by the uncertainty in $K(T)$ and $J(E)$. Using the 'universal' cross-section (Eqn (8)) for $K(T)$ will introduce small errors, particularly for multiple-scattered electrons, while evaluation of $K(T)$ from a dielectric response calculation[16] or from experimental REELS spectra[22] will introduce other uncertainties in $K(T)$.[8]

The measured spectrum $J(E)$ may be influenced by statistical noise and possible interference by close-lying peaks from other elements. These effects are most severe for spectra from deep layers, where the spectral intensity is diminished.

For analysis of model spectra, we have simulated the uncertainty in $K(T)$ by using the 'universal' cross-section. From this, we have found that the ability of the method to discriminate between different structures will depend on the actual situation. In general, the resolution in the determination of the detailed concentration depth profile is of the order of the inelastic mean free path λ. For the special case of island growth, it is thus possible to distinguish this growth mode from layer-by-layer growth (and vice versa) when the island height is $\gtrsim \lambda$ (see Figs 8 and 9). Similarly, concerning the determination of a layer-by-layer plus island surface structure, we have found that, depending on the combination of layer width and island height, it may or may not be possible to distinguish between pure island growth and layer-by-layer plus island growth.

In such cases where we cannot, by the analysis, discriminate between two different surface structures, the total amount of material in the surface region of the solid as determined from these two surface structures is accurate to within 10–15%. This holds for all surface structures with parameters (DX, $DX1 \lesssim 4$–6λ and $0 \leqslant f_1 \leqslant 1$).

5. SUMMARY AND CONCLUSIONS

A method was presented by which detailed quantitative information on in-depth concentration profiles can be extracted through analysis of surface electron spectra.

For determination of the inelastic background-corrected spectrum $F(E, \Omega_D)$, the central formula is Eqn (10). In Eqn (10), P_1 and $P(s)$ are given by Eqns (9) and (7). $\Sigma(s)$ entering Eqn (7) is given by Eqn (3), where λ may be taken from existing tabulations and the 'universal' cross-section in Eqn (8) may, for most solids, be used as an approximation for $K(T)$ (see discussion following Eqn (8)). The concentration depth profile is given by $f(x)$.

For several important classes of depth profiles, analytic expressions for $P(s)$ and P_1 were found in Section 3. The resulting integrals are evaluated by fast Fourier transformation.

If Eqn (10) is used in the analysis of a single spectrum, the form of $f(x)$ can be determined by the requirement that $F(E) \simeq 0$ in an energy region (e.g. from 40 to 100 eV) below the peak energy.

If the spectrum from a sample with a well-known depth distribution (e.g. a pure, homogeneous sample) is included in the analysis, the requirement used is that $F(E)$ is close to the $F(E)$ determined from the pure and homogeneous sample. Then, $f(x)$ is determined on an absolute scale. All information is thus extracted from only one or two experimental spectra. The method is therefore fast and non-destructive.

REFERENCES

1. S. Tougaard and P. Sigmund, *Phys. Rev.* **B25**, 4452 (1982).
2. A. Tofterup, *Surf. Sci.* **167**, 70 (1986).
3. V. M. Dwyer and J. A. D. Matthew, *Surf. Sci.* **193**, 549 (1988).
4. O. A. Baschenko and V. I. Nefedov, *J. Electron Spectrosc. Relat. Phenom.* **27**, 109 (1982).
5. R. Shimizu and S. Ichimura, *Surf. Sci.* **133**, 250 (1983).
6. A. Jablonski, *Surf. Interface Anal.*, **14**, 659 (1989).
7. A. Jablonski, *Surf. Sci.* **188**, 164 (1987).
8. S. Tougaard, *Surf. Interface Anal.* **11**, 453 (1988).
9. S. Tougaard, *Appl. Surf. Sci.* **32**, 332 (1988).
10. S. Tougaard, *Surf. Sci.*, **216**, 343 (1989).
11. S. Tougaard, *Surf. Sci.* **139**, 208 (1984).
12. S. Tougaard, *J. Vac. Sci. Technol.* **A5**, 1230 (1987).
13. S. Tougaard and A. Ignatiev, *Surf. Sci.* **129**, 250 (1983).
14. S. Tougaard, *J. Vac. Sci. Technol.* **A5**, 1275 (1987).
15. H. S. Hansen and S. Tougaard, to be published.
16. S. Tougaard and B. Jørgensen, *Surf. Sci.* **143**, 482 (1984).
17. S. Tougaard, *Solid State Commun.* **61**, 547 (1987).
18. C. J. Powell, *J. Vac. Sci. Technol.* **A3**, 1338 (1985).
19. S. Tanuma, C. J. Powell and D. R. Penn, *Surf. Interface Anal.* **11**, 577 (1988).
20. M. P. Seah and W. A. Dench, *Surf. Interface Anal.* **1**, 2 (1979).
21. R. H. Ritchie and A. Howie, *Philos. Mag.* **36**, 463 (1977).
22. S. Tougaard and I. Chorkendorff, *Phys. Rev.* **B35**, 6570 (1987).
23. S. Tougaard, *Phys. Rev.* **B34**, 6779 (1986).
24. E. Oran Brigham, *The Fast Fourier Transform*, Prentice-Hall, Englewood Cliffs, NJ (1974).
25. J. A. Venables, G. D. T. Spiller and M. Hanbücken, *Rep. Prog. Phys.* **47**, 399 (1984).
26. S. Doniach and M. Sunjic, *J. Phys.* **C3**, 285 (1970).